Contents lists available at ScienceDirect

Polymer Testing

POLYMER TESTING

ROGER BROWN

Material Properties

Microstructural and mechanical characterization of PA12/MWCNTs nanocomposite manufactured by selective laser sintering

Gean V. Salmoria [a,*], Rodrigo A. Paggi [a], Alexandre Lago [a], Valter E. Beal [b]

[a] CIMJECT, Departamento de Engenharia Mecânica, Universidade Federal de Santa Catarina, 88040-900 Florianópolis, SC, Brazil
[b] SENAI-CIMATEC, Serviço Nacional de Aprendizagem Industrial, Salvador, BA, Brazil

ARTICLE INFO

ABSTRACT

To determine the potential properties of commercial polyamide 12 (PA12) used in the selective laser sintering (SLS) process, multi-walled carbon nanotubes (MWCNTs) were dispersed in the polyamide powder by mechanical mixing to prepare a composite (PA/MWCNTs). Specimens of PA12 and PA/MWCNTs were manufactured by the SLS process. Infrared spectroscopy, X-ray diffraction and dynamic mechanical analysis were used to assess the structural and mechanical properties of the materials. Stress-strain tests showed higher values for flexural modulus and ultimate strength for the composite when compared to PA12 specimens. Changes in the viscoelastic properties suggest intermolecular interaction between the PA12 and MWCNTs. Fatigue tests show an improvement in the composite strength with the addition of MWCNTs, retarding the creep failure mechanism.

1. Introduction

Carbon nanotubes (CNTs) belong to a special class of materials. Their unique physical properties are attractive, particularly their mechanical and electrical characteristics, which include a high mechanical modulus (1 TPa), strength of 1 GPa and π electronic conductivity of 100 S/cm [1]. The incorporation of multi-walled carbon nanotubes (MWCNTs) into polymer matrices can improve the mechanical properties with effective load transfer between the matrix and the nanotubes. The particular properties of the composites are due to the aspect ratio of CNTs which have diameters in the range of a few nanometers and lengths of several micrometers [2,3].

Polyamide has been regarded as one of the most important engineering polymers due to its good processability, mechanical properties and thermal stability. Nanocomposites of polyamide and carbon nanotubes are promising for specific applications, for example in aerospace and aeronautic materials which require low weight and high mechanical strength.

Selective laser sintering (SLS) is a rapid manufacturing technology that can be applied to build parts from polymers, ceramics and metals. The process uses a laser that sinters selectively thin layers of powder spread over a moving platform. This technique has become a very useful tool for obtaining complex polymeric parts directly from software (CAD) designs in different material compositions with different properties [4–8].

Many studies have been dedicated to the evaluation of the mechanical and electromagnetic properties of nanocomposites prepared with carbonyl thermoplastics and carbon nanotubes. The composites are generally obtained by solution blending, melt mixing, electrospinning or in situ polymerization [9–12].

To evaluate the potential properties of commercial polyamide 12 (PA12) used in the SLS process, multi-walled carbon nanotubes (MWCNTs) were dispersed in the polyamide powder by mechanical mixing. Specimens of

* Corresponding author. Tel.: +55 48 3721 9387; fax: +55 48 3721 7615.
E-mail address: gsalmoria@emc.ufsc.br (G.V. Salmoria).

PA12 and the PA/MWCNT composite were manufactured by the SLS process and characterized by dynamic mechanical tests, X-ray diffraction (XRD) and scanning electron microscopy (SEM).

2. Experimental procedure

2.1. Materials

Multi-walled carbon nanotubes produced by MER Corp. were used in this study. The carbon nanotubes were obtained by chemical vapor deposition (CVD) and, according to the manufacturer's specifications, have average diameter of 140 ($\pm$30) nm, length of 7 ($\pm$2) μm and purity level higher than 90%. The polyamide 12 used as the matrix was Dura-Form (PA-Duraform) manufactured by 3D Systems Corporation. According to the material data sheet [13], the melting point is 184 °C with an average particle size of 58 μm.

2.2. Preparation of specimens

Composites with 0.5% (wt) of multi-walled carbon nanotubes were dispersed in polyamide powder by mechanical mixing using a cylindrical blender for 70 min at 90 rpm. Specimens were built by SLS using optimized processing parameters from previous factorial analysis based on mechanical behavior. The specimens were manufactured using a CO_2 laser with power of 3.8 W, a 250 μm focused beam diameter and scan speed of 44.5 mm/s. The building layer thickness used was 200 μm and the spacing between the laser scans was 125 μm. The pure PA12 and composite specimens were manufactured using the same processing parameters.

2.3. Raman and infrared spectroscopy

Raman spectra were obtained with a Renishaw inVia Raman microscope, equipped with an argon laser (514 nm). For the data acquisition, 100% of laser power was used with three accumulations in order to obtain a significant curve. The range scanned was 100–3500 cm^{-1}. Infrared spectra of PA12 and MWCNTs were obtained using a 16 PC Perkin Elmer spectrophotometer, performing 20 scans at a resolution of 4 cm^{-1} using KBr plates, in order to evaluate the polymer absorbance at the CO_2 laser wavelength.

2.4. Mechanical analysis

Mechanical analysis was performed on a TA Instruments model Q800 analyzer in single cantilever mode. Flexural tests were conducted and stress-strain curves were obtained at a loading rate of 2 N min^{-1} and 30 °C. From dynamic mechanical analysis, the storage modulus (E') and the loss factor ($\tan \delta = E'/E''$) at a fixed frequency of 1 Hz were determined in the temperature range of -50–125 °C with a heating rate of 3 °C min^{-1}. Fatigue experiments were conducted at 30 °C and 1 Hz applying 50% of the maximum strain amplitude determined from the stress versus strain curves for each specimen.

2.5. X-ray diffraction (XRD) and scanning electron microscopy (SEM)

The X-ray diffraction measurements were performed using a Philips PW1150 vertical diffractometer. The Cu–Ka nickel filtered radiation was detected in the range of 6–60°. The results of this analysis were used to determine the microstructure of the specimens. The specimens were inspected with a Phillips XL30 scanning electron microscope in order to investigate the fracture surface, nanotube dispersion and microstructure. The specimens were coated with gold in a Bal-Tec Sputter Coater SCD005.

3. Results and discussion

Fig. 1 shows the micrographs of the PA powder (a) and the MWCNTs (b) used in this investigation. Fig. 2 shows the Raman spectra acquired for the MWCNTs. The peak at 1350 cm^{-1} (D band) is related to sp^3 bonds and the peak at 1580 cm^{-1} (G band) to the sp^2 bonds of the MWCNTs. The peak at 2700 cm^{-1} (G1′ band) is characteristic of carbon nanotubes in analyses using an argon laser.

The degree of integrity of the MWCNTs structure can be evaluated from the ratio of D to G bands [14]. This ratio for the MWCNTs analyzed was 0.145, indicating a low degree of defects present in the structure of the carbon nanotubes used in this study.
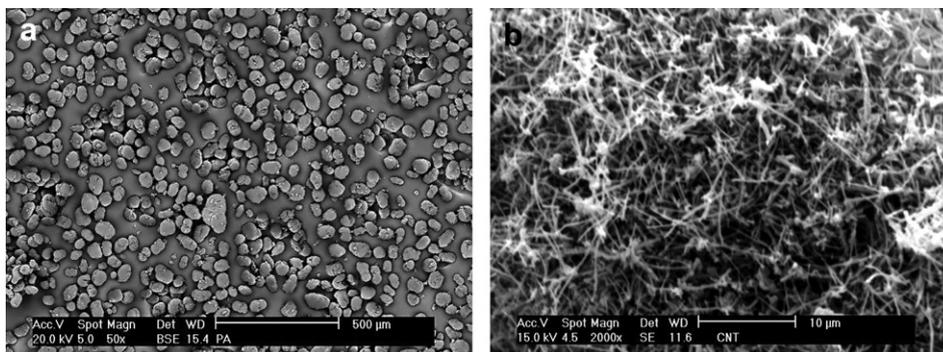

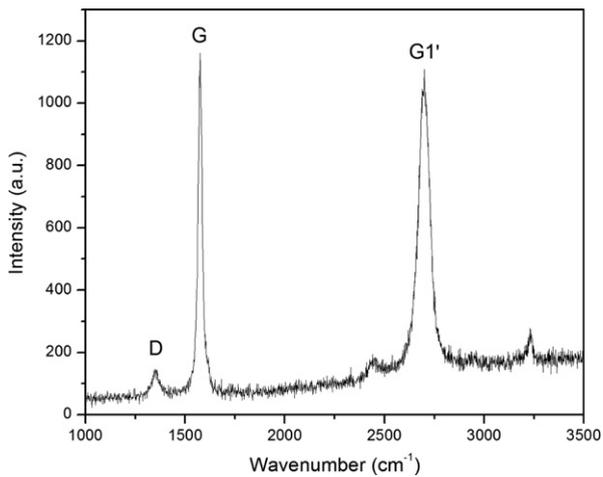**Fig. 1.** Micrographs of PA12 particles (a) and MWCNTs (b).

Fig. 2. Raman spectrum of MWCNTs.

Fig. 4. X-ray diffraction patterns of PA12 and PA12/MWCNTs composite.

Fig. 3 shows the infrared spectra of PA12 and MWCNTs from 500 to 4000 cm^{-1}. The highlighted regions are the irradiation band used in CO_2 laser processing with a wavelength of 10.2 μm. The presence of peaks related to C-N bonds in PA12 at 1000 cm^{-1} ensures effective absorption of CO_2 laser energy and sintering. The high absorption of CO_2 lase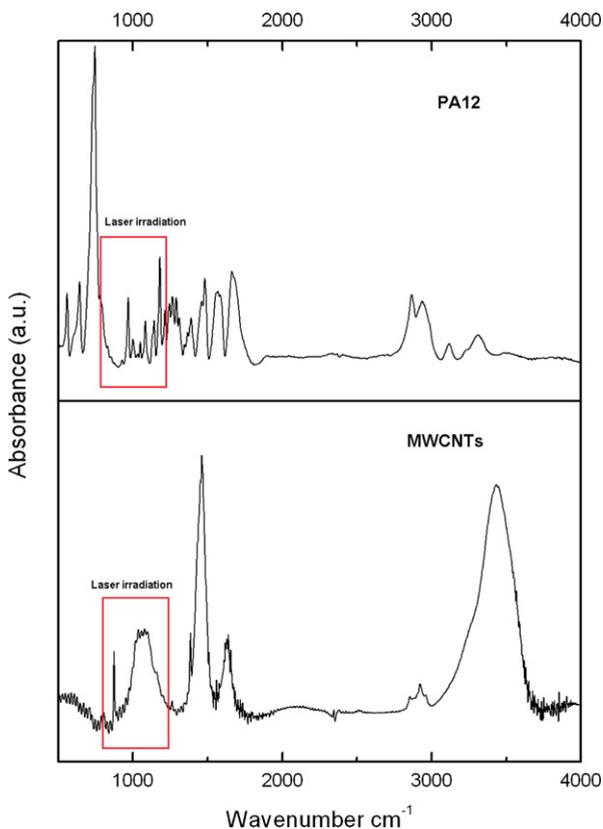r energy by MWCNTs during composite sintering can be explained by the presence of an absorption band at 1000 cm^{-1} related to C=C asymmetry vibration in the MWCNT spectrum.

The X-ray diffraction patterns in Fig. 4 show that sintered PA12 and composite specimens present only a reflection peak at 21° relating to the γ phase. The γ phase is not thermodynamically stable, being predominant under fast cooling conditions such as laser sintering [15].

Table 1 gives a summary of the flexural mechanical properties determined in the stress-strain test. The addition of 0.5% of carbon nanotubes promoted a 10% increase in tensile strength and a reduction in the elongation (11–9%) of the composite in comparison to the pure PA12. In the PA12/MWCNT composite, the loading is mainly borne by the matrix. The MWCNTs dispersed in the matrix inhibit the movement of the molecular chains, which explains why the ultimate strength of the PA12/MWCNT composite was higher than that for the pure PA12. Nevertheless, the addition of MWCNTs can increase defects in sintered specimens, which explains the larger deviation in the values for the mechanical properties of the composite when compared to the pure PA12 values.

Fig. 5 shows the micrographs for the fracture surface of PA12 (a) and PA12/MWCNTs (b). The fractured specimen surfaces demonstrated that the addition of 0.5% MWCNTs generated a specimen of greater density with the presence of defects when compared to the PA specimen. These results are probably due to the high absorption of laser energy by the MWCNTs and the coalescence of melted PA. The composite fracture surface shows evidence of brittle failure with a clear origin in the supra-central position, confirming the increased rigidity of the composite.

Fig. 3. Infrared spectra of PA12 and MWCNTs.

Table 1
Flexural mechanical properties of PA12 and the PA12/MWCNTs composite.

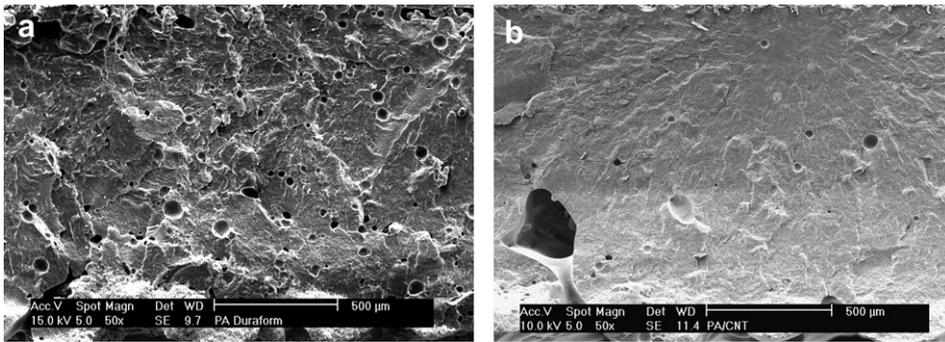|	DuraForm PA	PA/MWCNT
Ultimate strength (MPa)	86 ± 5	94 ± 9
Flexural modulus (MPa)	546 ± 28	718 ± 125
Elongation (%)	11 ± 0.5	9 ± 1.5

Fig. 5. Micrographs of cryogenic fracture surface of PA12 (a) and PA12/MWCNTs composite (b).
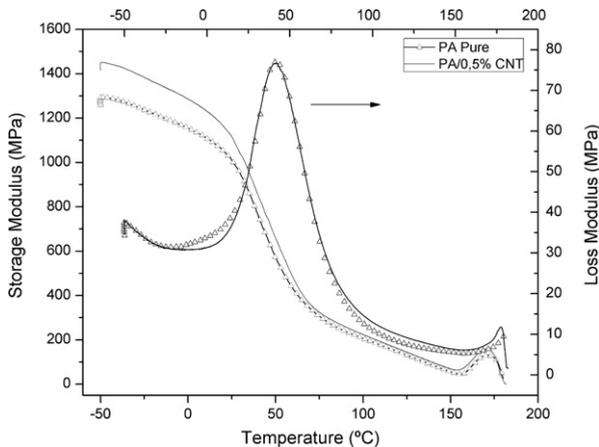

Fig. 6. Storage (E′) and loss (E′) moduli as a function of temperature for PA12 and the PA12/MWCNTs composite.

In order to evaluate the viscoelastic properties of the PA12 and composite specimens, DMA analysis were carried out. The variations in the storage (E′) and loss (E″) moduli with temperature are shown in Fig. 6. The storage modulus

Fig. 7. Fatigue strength as a function of cycle number for PA and PA/MWCNTs composite.

or elastic component (E′) of the composite presented different values for the plateau observed in the glassy region (below the Tg), from approximately −50 to 20 °C. The average increase in the storage modulus was 12% with the addition of 0.5% of MWCNTs. According to Satapathy et al. [16], the relative difference in the molecular mobility of the polymer segments in the vicinity of the nanotubes compared with the bulk polymer can cause a significant difference between the viscoelastic responses of the pure PA and the MWCNTs-reinforced composite. The maximum value for the loss modulus or viscous component (E″) gives information on the glass transition temperature. The addition of 0.5% of MWCNTs to PA12 changed the initial relaxation of the PA chain segments, retarding the dissipation phenomenon observed through an increase in E″. This suggests that there is a secondary interaction between the MWCNTs and PA12, probably via a π-carbonyl electronic system, which can modify the mobility of polymer chains.

The results of fatigue tests for PA12 and PA12/MWCNTs are shown in Fig. 7. A decrease in the stiffness as a function of the number of cycles was observed for PA12 and the composite under the same test conditions. Pure PA12 showed a lower stiffness in the fatigue test than the PA12/MWCNTs composite, suggesting that the carbon nanotubes were responsible for reducing the molecular mobility of the polymeric chains and retarding the creep failure.

4. Conclusions

Stress-strain analysis showed high values for the flexural modulus and ultimate strength for the PA12/MWCNTs composite when compared to PA12 specimens. The average increase in the storage modulus with addition of 0.5%wt of MWCNTs was 12%. The addition of 0.5% of MWCNTs to the PA12 changed the initial relaxation of the PA chain segments, suggesting the existence of a secondary interaction between the MWCNTs and PA12. The fatigue test showed an improvement in the composite stiffness with the addition of MWCNTs, retarding the creep failure mechanism and improving the dynamic mechanical properties of the PA12/MWCNTs composite. The addition of MWCNTs to PA12 led to amelioration of the PA properties, permitting the use of SLS to manufacture new functional parts with potential mechanical and electromagnetic applications.
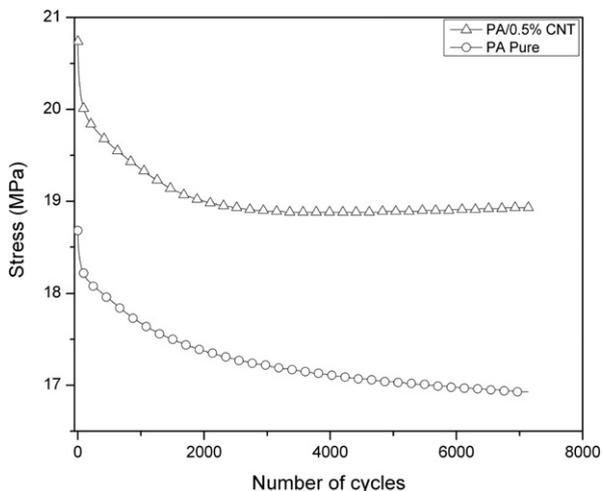
Acknowledgements

References

[1] C.J. Ko, C.Y. Lee, F.H. Ko, H.L. Chen, T.C. Chu, Microelectronic Eng. 73-74 (2004) 570–577.
[2] M.V. Jose, B.W. Steinert, V. Thomas, D.R. Dean, M.A. Abdalla, G. Price, et al., Polymer 48 (2007) 1096–1104.
[3] R. Mulhaupt, T. Engelhardt, N. Schall, Nanocomposites – auf dem weg zur anwendung, Kunststoffe 91 (2001) 178–190.
[4] G.V. Salmoria, J.L. Leite, C.H. Ahrens, A. Lago, A.T.N. Pires, Polym. Test. 26 (2007) 361–368.
[5] G.V. Salmoria, J.L. Leite, R.A. Paggi, A. Lago, A.T.N. Pires, Polym. Test. 27 (2008) 657–659.
[6] G.V. Salmoria, C.H. Ahrens, P. Klauss, R.A. Paggi, R.G. Oliveira, A. Lago, Mater. Res. 10 (2007) 211–214.
[7] G.V. Salmoria, J.L. Leite, C. Lopes, R.A.F. Machado, A. Lago, Advanced Research in Virtual and Rapid Prototyping. Taylor & Francis, London, 2007, 305–311.
[8] G.V. Salmoria, J.L. Leite, C.H. Lopes, R.A. Paggi, A. Lago, Advanced Research in Virtual and Rapid Prototyping. Taylor & Francis, London, 2007, 313–317.
[9] L. Li, C.Y. Li, C. Ni, L. Rong, B. Hsiao, Polymer 48 (2007) 3452–3460.
[10] A. Eitan, F.T. Fisher, R. Andrews, L.C. Brinson, L.S. Schadler, Compos. Sci. Tech. 66 (2006) 1162–1173.
[11] Z. Li, G. Luo, F. Wei, Y. Huang, Compos. Sci. Tech. 66 (2006) 1022–1029.
[12] A. Yu, H. Hu, E. Bekyarova, M.E. Itkis, J. Gao, B. Zhao, et al., Compos. Sci. Tech. 66 (2006) 1190–1197.
[13] DuraForm^{TM} material data sheet.
[14] E.F. Antunes, A. Lobo, E.J. Corat, V.J. Trava-Airoldi, A.A. Martin, C. Veríssimo, Carbon 44 (2006) 2202–2211.
[15] R. Androsh, M. Stolp, H.J. Radusch, Thermochim. Acta 271 (1996) 1–8.
[16] B.K. Satapathy, R. Welsch, P. Potsche, A. Janke, Compos. Sci. Tech. 67 (2007) 867–879.